COMPARATIVE PERFORMANCE OF TIME–FREQUENCY BASED EEG SPIKE DETECTION TECHNIQUES

Hamid Hassanpour, Luke Rankine, Mostefa Mesbah and Boualem Boashash

Signal Processing Research Centre, Queensland University of Technology
GPO Box 2434, Brisbane, QLD 4001, Australia
E-mail: h.hassanpour@ieee.org

ABSTRACT

This paper investigates the performance of time–frequency based EEG spike detection techniques. The nonstationary nature of EEG makes time-frequency methodology a suitable tool for analysis. The high instantaneous energy of spikes are reflected as very localised energy patterns in the time-frequency domain with reduced time duration toward the high frequency area. These characteristics of spikes in the time-frequency domain makes them recognisable from the background. Two recently published spike detection methods, based on quadratic time-frequency and adaptive time-frequency parameterisation are considered in this investigation. These methods have been applied on both synthetic and real EEG signals. The obtained results show the superior performance of the quadratic time-frequency method for detecting EEG spikes in terms of resolution and robustness to noise.

1. INTRODUCTION

The electroencephalogram (EEG) is an invaluable measurement for monitoring brain activity [1]. Brain functioning affects the morphology of EEG. Consequently, seizures, which are a kind of brain abnormality, can be detected using spikes and their firing pattern in EEG [2]. In this application, performance of the seizure detection technique depends on the accuracy of the spike detection algorithm.

In the context of EEG, spikes can be defined as transient signals, clearly distinguishable from the background activity with a duration ranging from 20 to 70 msec [3]. Hence, spikes are nonstationary short–time broadband signals with high instantaneous energy [4]. Spike detection in nonstationary signals, such as EEG, is a challenging problem. Detection methods based on the assumption that the background signal is stationary or quasi-stationary (as assumed in [4, 5]) are not appropriate for these type of signals.

The nonstationarity of EEG makes time-frequency distributions (TFDs) a suitable tool for spike detection. As spikes are short time broadband events, they are represented as ridges in the time–frequency (TF) domain. In this domain, the high instantaneous energy of spikes allows them to be distinguishable from the background [6] (see Figure 1). As can be seen, in this domain spikes are represented as highly localised energy pattern especially in the high frequency area.

There are several EEG spike detection methods in the literature, for example [4, 6, 7, 8]. It has previously been shown that the TF-based methods are superior to the time domain based approach [9]. The aim of this paper is to compare the performance of the two most recently published TF-based EEG spike detection methods, namely quadratic TF (QTF) [6] and adaptive TF parameterisation (ATFP) [8], using both synthetic and real EEG signals.

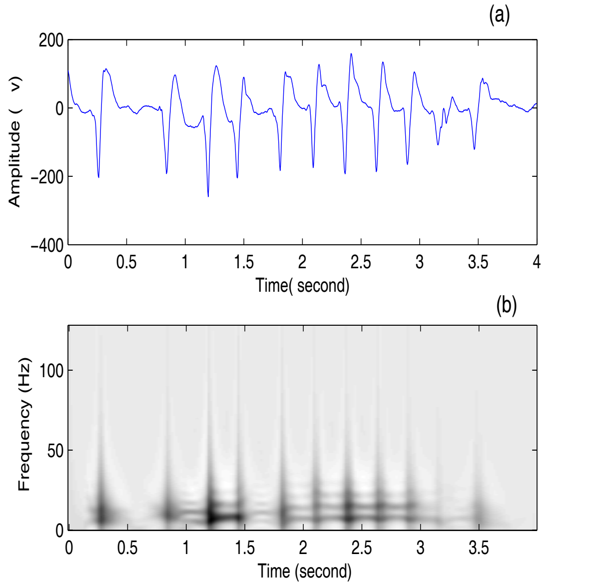

Figure 1: EEG data containing epileptic spikes: (a) Time domain, (b) TF domain (using a quadratic TFD).

2. REVIEW OF TF-BASED SPIKE DETECTION TECHNIQUES

2.1 The ATFP technique

This approach uses the matching pursuit (MP) atomic decomposition technique. MP is an algorithm for which a signal representation can be obtained using a redundant collection of waveforms (atoms), , generally referred to as a dictionary [10]. MP builds up a signal representation iteratively by finding the atom at each iteration for which the projection of the remaining signal energy is maximum. The MP representation of a signal, s, using m atoms is shown as

$$s = \mathop{}_{i=0}^{m-1} \langle R^i s, \quad {}_i \rangle \quad {}_i + R^i m \qquad (1)$$

where $R^i s$ is the representation error after i iterations and $\langle \cdot, \cdot \rangle$ is the inner product function.

The dictionary used in this paper is a redundant Gabor time-frequency dictionary . The Gabor atoms (t) are indexed by the vector of parameters $= [s, \ , \ ]$, which respectively relate to the dilation, translation and modulation transformations of a Gaussian function (t). Therefore, MP decomposition provides a time-frequency parameterisation of a signal [8].

Signal spikes, which are characterized by high energy and short time duration, are represented as atoms with a significantly high coefficient value and small scale parameter when using MP. Temporal information related to the spike can then be obtained from the translation parameter. Therefore, by setting a threshold for the atom scale parameter and atom coefficient value, signal spikes can be detected using MP time-frequency parameterisation.

2.2 The QTF technique

In this approach the signal of interest is first mapped to the TF domain using a quadratic time-frequency distribution (TFD). The TFD of a signal can be thought of as a joint representation of both time and frequency domains of the signal energy density. For a given signal, $s(n)$, its TFD can be expressed as [11]:

$$_z(t,f) = \int_{-} \int_{-} \int_{-} \begin{array}{l} e^{j2 \ v(u-t)} g(v, \ ) z(u + \frac{}{2}) \\ z^*(u - \frac{}{2}) e^{-j2 \ f} \ dv du d \end{array} \quad (2)$$

where $z(n)$ is the analytic signal associated with $s(n)$, and $g(v, \ )$ is a 2–dimensional kernel that determines the characteristics of the TFD. For example, by setting $g(v, \ ) = 1$ we get the Wigner-Ville distribution (WVD).

One problem inherit with quadratic TFDs, particularly WVD, are cross-terms, which are a result of the quadratic nature of the transformation. Cross-terms can make interpretation of the time-frequency representation difficult. In order to reduce the effect of cross-terms, the Choi-Williams distrribution (CWD) is used. The CWD is a member of the reduced interference TFD class of quadratic TFDs [12]. The CWD is defined by setting the kernel $g(v, \ )$ in Eq. (2) to $e^{-v^2 \ ^2/}$ where is a smoothing parameter (≥ 0) [12].

In the QTF technique, the TFD is then enhanced by low-pass filtering the singular vectors of the TFD matrix. The enhancement process using the SVD-based technique attenuates the effects of noise in the TFD of the signal [13].

Once the TFD of the signal has been enhanced, two relatively high frequency slices are extracted. If both frequency slices have any spike signature at the same position, the related time domain signal is judged to contain spike at that position. Spikes in these frequency slices appear as local maxima, which are well localised in time. To further amplify these signatures, the smoothed nonlinear energy operator (SNEO) is applied to the frequency slices [4]. Assuming that the nonlinear energy operator is applied to the time-series $x(t)$ representing a given TFD frequency slice, the output is given by:

$$[x(t)] = x^2(t) - x(t+1)x(t-1) \quad (3)$$

To further enhance the localisation of the local maxima, $(.)$ is smoothed using a Bartlett window. Values of the smoothed $(.)$ are then thresholded to keep only the more energetic local maxima.

3. PERFORMANCE COMPARISON

The performance of the two above mentioned techniques in detecting EEG spikes have been evaluated using both synthetic and real life EEG signals as described in the following sections.

3.1 Synthetic Newborn EEG signal

To simulate newborn EEG signals containing spike events the following synthetic signal model is used:

$$x(t) = h(t) + s(t), \quad (4)$$

where $h(t)$ and $s(t)$ are the spike train set and the background EEG signal, respectively. The background $s(t)$ is a normal newborn EEG signal simulated using fractal dimension (FD) theory [14]. To create a fractal signal with a known FD we start with a complex Hermitian sequence, $S_w(f)$, with constant amplitude over all f. This sequence is representative of white Gaussian noise in the Fourier domain, which can be represented by

$$S_w(f) = r(f)e^{j \ (f)}, \quad (5)$$

where r and refer to the magnitude and phase of the sequence, respectively. For white Gaussian noise the chosen phase sequence should be uniformly distributed over $[0, 2 \ )$. However, because of the Hermitian symmetry of $S_w(f)$ only half of the phase sequence needs to be randomly selected as this will also define the second half of the phase sequence. This sequence can then be multiplied by the power law sequence that relates to the desired FD to give the power spectrum of the fractal signal

$$S_F(f) = S_w(f) \cdot \frac{1}{|f|} = r_F(f)e^{j \ (f)}, \quad (6)$$

where r_F is the new magnitude sequence of the fractal signal. The Fourier transform of the fractal signal is then given as

$$\mathscr{F}_F(f) = \sqrt{r_F(f)}e^{j \ (f)}. \quad (7)$$

To obtain the fractal signal in the time domain we take the inverse Fourier transform of (7), such that

$$s_F(t) = \int_{-} \mathscr{F}_F(f)e^{j2 \ ft} df. \quad (8)$$

To simulate newborn EEG data, the next step is to high pass filter the fractal signal to remove insignificant power in frequencies less than 0.5Hz [15]. The high pass filtering may affect the FD of the signal. However, it was shown that the FD estimate of the filtered signal is approximately the FD estimate of the non-filtered signal in FD from 1.25 to 1.65, for which a large proportion of the real EEG is estimated [14].

To consider nonstationarity in EEG, we chose to create synthetic epochs of length 256 samples. The theoretical FD of each epoch is randomly chosen according to a normal distribution with a mean of 1.525 and standard deviation of 0.1 [14]. The epochs were then high pass filtered with cutoff

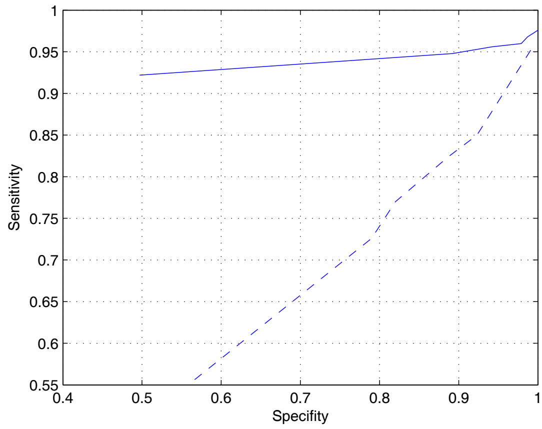

Figure 2: ROC curves showing performance of the QTF (solid line) and ATFP (dashed line).

frequency randomly selected according to a normal distribution on the interval $[0.4, 0.65]$Hz. The highpass filtering then gave a varying peak frequency approximately between $[0.4, 0.65]$Hz. The synthetic epochs were then concatenated to form the synthetic signal. By forming epochs with varying FD and high pass cutoff frequencies, the signal will have a time-varying spectrum. This means that the simulated EEG signals will be non-stationary which is a characteristic of the EEG.

After simulating the background signal, the spikes in $h(t)$ are distributed randomly over the background signal. The spikes are taken as triangular symmetric pulses with random signs, widths which range between 20 and 70msec, and amplitudes uniformly distributed between 2.5 and 5.5. The signal is sampled at a rate of 128 Hz ($F_s = 128Hz$).

For the purpose of statistically evaluating the two TF-based spike detection techniques and comparing their performance, multiple $x(t)$ (see (3)) were created. The signals $x(t)$ were created with a spike train set $h(t)$ to background $s(t)$ ratio (SBR), shown as

$$\mathrm{SBR} = 10\log_{10}\left(\frac{\int_{-} |h(t)|^2 dt}{\int_{-} |s(t)|^2 dt}\right),$$

ranging between [-7.5,7.5]dB with 100 realisations of $x(t)$ for each SBR. In these simulations the spike train set had 5 randomly distributed spikes (using a uniform distribution).

The detection of spikes using ATFP technique required setting threshold values for the scale parameter and the coefficient value. Our detection method required an atom to have a scale width between 20 and 100ms for a spike to be detected. This range is slightly larger than the definition of a spike in the literature. However, this scale range gave the best results. Also, to obtain good results for various SBR the threshold for atom coefficient values was set between $[0.06, 0.14] * ||x(t)||_2$, where $|| \cdot ||$ denotes the ℓ^2 norm, 0.06 and 0.14 are for the lowest and highest SBR respectively.

To detect spikes using the QTF, two frequency slices are extracted around $60Hz$ and $68Hz$. The sharp local maxima, twice higher than the median value of the frequency slices, represent the position of spikes in the time domain. In this approach a spike is considered to exist if its signature is detected at the same position in both frequency slices.

The accuracy of these techniques may be measured by considering their sensitivity R_{sn} and specificity R_{sp} as follows:

$$R_{sn} = \frac{TP}{TP+FN}$$

$$R_{sp} = 1 - \frac{FP}{TP+FP} \quad (9)$$

where TP, FN, and FP respectively represent true positive, false negative and false positive detection rates. Figure 2 shows the Receiver Operating Characteristic (ROC) curves of the performance values using (4) with SBR chosen between $-7.5dB$ and $7.5dB$, and 100 realisations for each selected SBR. The figure shows that QTF has a better performance compared to the ATFP specifically in the area with a lower specificity which correspond to a lower SBR. These results indicate that the QTF-based method is more robust to background EEG amplitude than the ATFP-based method.

3.2 Real Adult EEG signal

To compare the performance of the two techniques on real EEG, data from http://republika.pl/eegspike were used, which were provided by the authors of [16]. This dataset contains 51 4-second epochs containing epileptic spikes. All of these epochs were used in this assessment.

The parameters for ATFP were redefined for this dataset. The scale parameter for a spike/ sharp wave to be detected was set between 25-120 msec. The amplitude threshold was set at 300 a.u. [8] (i.e. arbitrary units related to the signals in http://republika.pl/eegspike).

In detecting spikes of the real EEG data using the QTF, similar with the synthetic signal, we used two frequency slices extracted around $60Hz$ and $68Hz$. A spike is considered to exist if its signature is detected at the same position in both frequency slices.

The 51 epochs of the dataset had 145 epileptic spikes in total. Table 1 represents the performance results of the two spike detection techniques applied to these dataset. Using Eq. (9) the ATFP yielded sensitivity 0.66 and specifity 0.74, while the QTF resulted sensitivity 0.93 and specifity 0.94. Both of the techniques provide high TF resolution, however, the ATFP fails to detect successive spikes that are close together. In such case, the successive spikes are considered as a periodic pattern and hence they are represented by atoms with scale parameters longer than that which is indicative of spike occurrence.

Parameters	*ATFP*	*QTF*
TP	65.5%	93.1%
FP	23.4%	6.2%
FN	34.4%	6.8%

Table 1: The ATFP and QTF performance results using the real EEG signals.

Figure 3 shows the TF representation of the EEG data displayed in Figure 1(a) using the MP decomposition. The TF representation is obtained by the superposition of the

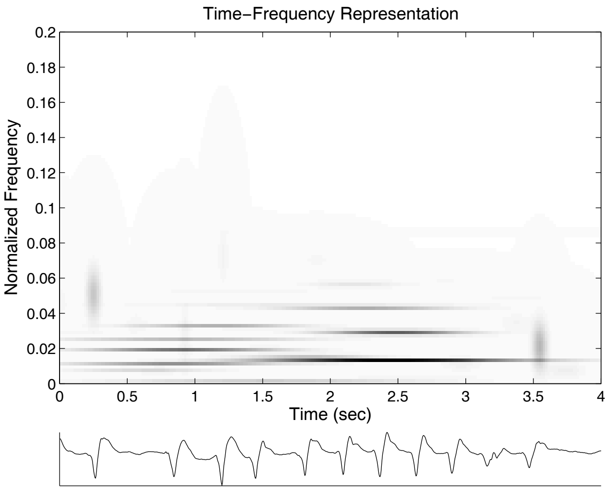

Figure 3: TF representation of the EEG data displayed in Figure 1(a) using the MP.

WVD of Gabor atoms selected for the representation such that

$$E_s(t,f) = \sum_{i=0}^{m-1} |\langle R^i s, g_{\gamma_i}\rangle|^2 WVD_{g_{\gamma_i}}(t,f) \qquad (10)$$

Horizontal lines in the TF plot are representations for successive spikes which were considered as periodic patterns. Our observations indicate that the ability of ATFP to detect periodic spikes is highly dependent on the time interval between successive spikes. These successive spikes are clearly recognisable using the QTF representation (see Figure 1).

4. CONCLUSION

Performance comparison of two time-frequency based techniques, namely quadratic time-frequency and adaptive time-frequency parameterisation, for detecting epileptic spikes has been performed using both synthetic and real EEG data. Robustness of the techniques to noise and their resolution in detecting adjacent spikes have been investigated in this paper. Results on synthetic EEG indicate that the technique based on the quadratic time-frequency is more robust to background EEG amplitude than the other technique. Also, this technique is better in detecting successive spikes which are close in time, while the other technique may consider these spikes as periodic patterns and hence fail to recognise them.

REFERENCES

[1] Eli M. Mizrahi and Peter Kellaway, "Neonatal electrocephalography," in *Diagnosis and management of neonatal seizures*, pp. 99–143. Lippincott-Raven, 1998.

[2] H. Hassanpour and M. Mesbah, "Neonatal EEG seizure detection using spike signatures in the time-frequency domain," *IEEE Int. Sympo. on Sig. Proc. and Its Appl. (ISSPA)*, vol. 2, pp. 41–44, Paris, France, July 2003.

[3] P. Y. Ktonas, "Automatic spike and sharp wave (SSW) detection," in *Methods of Analysis of Brain Electrical and Magnetic Signals*, A. Gevins and A. Remond, Eds., vol. 1, pp. 211–241. Elsevier, Amsterdam, 1987.

[4] S. Mukhopadhyay and G. C. Ray, "A new interpretation of nonlinear energy operator and its efficiency in spike detection," *IEEE Trans. on Biomed. Eng.*, vol. 45, no. 2, pp. 180–187, Feb. 1998.

[5] G. Calvagno, M. Ermani, R. Rinaldo, and F. Sartoretto, "A multiresolution approach to spike detection in EEG," *IEEE Int. Conf. Acoustic, Speech and Sig. Proc.*, vol. 6, pp. 3582–3585, 2000.

[6] H. Hassanpour, M. Mesbah, and B. Boashash, "EEG spike detection using time-frequency signal analysis," *the IEEE Int. Conf. on Acoustics, Speech, and Signal Processing, Montreal, Quebec, Canada*, vol. 5, pp. V–421–V–424, 2004.

[7] E. Hulata, R. Segev, and E. Ben-Jacob, "A method for spike sorting and detection based on wavelet packets and shannon's mutual information," *Journal of Neuroscience Methods*, vol. 117, pp. 1–12, 2002.

[8] Durka P. J, "Adaptive time-frequency parametrization of epileptic spikes," *Physical Review E*, vol. 69, 051914, 2004.

[9] H. Hassanpour, M. Mesbah, and B. Boashash, "A time–frequency approach for spike detection," *10th IEEE Int. Conf. on Electronics, Circuits and Systems (ICECS)*, pp. 56–59, Sharjah, UAE, Dec. 2003.

[10] S.G. Mallat and Z. Zhang, "Matching pursuits with time-frequency dictionaries," *IEEE Trans. on Signal Processing*, vol. 41, no. 12, pp. 3397–3415, 1993.

[11] B. Boashash and A.P. Reilly, "Algorithms for time-frequency signal analysis," in *Time Frequency Signal Analysis - Methods and Applications*, B. Boashash, Ed., chapter 7. Longman Cheshire, 1992.

[12] H. I. Choi and W. J. Williams, "Improved time-frequency representation of multicomponent signals using exponential kernels," *IEEE Transactions on Acoustics, Speech and Signal Processing*, vol. 37, no. 6, pp. 862–871, 1989.

[13] H. Hassanpour, M. Mesbah, and B. Boashash, "SVD–based technique for enhancing the time–frequency representation of signals," *Fourth Australian Workshop on Sig. Proc. and Appl. (WoSPA)*, pp. 113–116, Brisbane, Australia, Dec. 2002.

[14] L. Rankine, H. Hassanpour, M. Mesbah, and B. Boashash, "EEG simulation using fractal dimension analysis," *Thirteen Iranian Conference on Electrical Engineering, (submitted)*.

[15] D. Schramm, B. Scheidt, A. Hübler, J. Frenzel, K. Holthausen, and O. Breidbach, "Spectral analysis of electroencephalogram during sleep-related apneas in pre-term and term born infants in the first weeks of life," *Clinical Neurophysiology*, vol. 111, pp. 1788–1791, 2000.

[16] M. Latka, Z. Was, A. Kozik, and B. J. West, "Wavelet analysis of epileptic spikes," *Physical Review E*, vol. 67, no. 052902, 2003.